6. R. E. Apfel, in *Ultrasonics: Methods in Experimental Physics*, P. D. Edmonds, Ed. (Academic Press, New York, 1981), vol. 19, pp. 356–413; E. A. Neppiras, *Phys. Rep.* **61**, 159 (1980).
7. M. A. Margulis and A. F. Dmitrieva, *Zh. Fiz. Khim.* **56**, 323 (1982); R. I. Nigmatulin *et al.*, *Int. J. Heat Mass Transfer* **24**, 1033 (1981).
8. D. F. Gaitan and L. A. Crum, in *Frontiers of Nonlinear Acoustics: 12th International Symposium on Nonlinear Acoustics*, M. Hamilton and D. Blackstock, Eds. (Elsevier, New York, 1990), pp. 459–463; A. Prosperetti *et al.*, *J. Acoust. Soc. Am.* **83**, 502 (1988); A. Prosperetti and A. Lezzi, *J. Fluid Mech.* **168**, 457 (1986); L. A. Crum and G. T. Reynolds, *J. Acoust. Soc. Am.* **78**, 137 (1985).
9. S. Fujikawa and T. Akamatsu, *J. Fluid Mech.* **97**, 481 (1980); Y. Matsumoto and F. Takemura, in *Cavitation and Multiphase Flow Forum*, O. Furuya, Ed. (ASME, New York, 1990), pp. 29–34.
10. Lord Rayleigh, *Philos. Mag.* **1917**, 34 and 94 (1917).
11. K. S. Suslick *et al.*, *J. Am. Chem. Soc.* **108**, 5641 (1986); K. S. Suslick *et al.*, *IEEE Trans. Ultrason. Ferroelectr. Freq. Control* **33**, 143 (1986); K. S. Suslick *et al.*, *IEEE Ultrason. Symp.* **1985**, 1116 (1985).
12. K. S. Suslick and E. B. Flint, *Nature* **330**, 553 (1987); E. B. Flint and K. S. Suslick, *J. Am. Chem. Soc.* **111**, 6987 (1989).
13. G. Marr, *Plasma Spectroscopy* (Elsevier, Amsterdam, 1968).
14. G. Herzberg, *Molecular Spectra and Molecular Spectra: Spectra of Diatomic Molecules* (Van Nostrand, New York, 1950) vol. I; K. P. Huber and G. Herzberg, *Molecular Spectra and Molecular Spectra: Constants of Diatomic Molecules* (Van Nostrand, New York, 1979), vol. IV.
15. A. Schadee, *Bull. Astron. Inst. Neth.* **17**, 311 (1964).
16. Attempts were made to record sonoluminescence spectra with a 2-m spectrograph equipped with a 1200-groove-per-millimeter grating and a charge-coupled device detector; the ratio of signal to noise was insufficient to provide usable spectra.
17. M. M. Smit-Miessen and J. L. Spier, *Physica (Amsterdam)* **9**, 193 (1942); *ibid.*, p. 442; J. L. Spier and J. A. Smit, *ibid.*, p. 587. In this approach, spectral substructure from *J*-value splittings and variations in electronic transition moment with ν'' are neglected.
18. J. C. McCallum *et al.*, *Spectroscopic Report No. 1* (York University Centre for Research in Experimental Space Science, York, U.K., 1970).
19. G. Stark and S. P. Davis, *Z. Phys. A* **321**, 75 (1985).
20. Attempts to model the CN violet ($B^2\Sigma - X^2\Sigma$) emission from the sonoluminescence of silicone oil under 20% N_2 in Ar were less successful. The experimental spectrum appeared to originate from molecules that were not fully thermally equilibrated. This is not unusual for CN formed from the extremely exothermic reaction of carbon atoms and nitrogen atoms [M. R. Gorbal and M. I. Savadatti, *J. Quant. Spectrosc. Radiat. Transfer* **26**, 457 (1981)].
21. Recent data indicate sonoluminescence lifetimes in water may be as short as 100 ps; given the high pressures during cavitation, thermal equilibration of C_2 is still likely (B. P. Barber and S. Putterman, *Nature* **352**, 318 (1991).
22. E. B. Flint and K. S. Suslick, *J. Phys. Chem.* **95**, 1485 (1991).
23. *Information about Silicone Fluids* and *Vapor Pressure Data of Dow Corning 200 Fluids*, available from C. Kovarik (Dow Corning, Midland, MI).
24. P. Kruus, M. O'Neill, D. Robertson, *Ultrasonics* **28**, 304 (1990); K. S. Suslick, J. W. Gawienowski, P. F. Schubert, H. H. Wang, *ibid.* **22**, 33 (1984); *J. Phys. Chem.* **87**, 2299 (1983).
25. We thank A. Scheeline, J. M. Lisy, and S. W. Rynders for useful discussions on the calculation of synthetic spectra. Supported by the NSF.

29 April 1991; accepted 29 July 1991

The Role of Magma Overpressure in Suppressing Earthquakes and Topography: Worldwide Examples

TOM PARSONS AND GEORGE A. THOMPSON

In an extending terrane basaltic magma supplied at a pressure greater than the least principal stress (overpressure) may be capable of suppressing normal faulting and the earthquakes and topographic relief that commonly accompany normal faulting. As vertical dikes intrude, they press against their walls in the direction opposite the least principal stress and increase its magnitude. The emplacement of tabular intrusions causes the internal magma pressure to act selectively in opposition to tectonic stresses. This process tends to equalize the stresses and thus diminishes the deviatoric stress (difference between maximum and minimum stresses) that creates faults and causes earthquakes. Observations of the pattern of seismicity and magmatism worldwide indicate that magmatism commonly supplants large earthquakes as the primary mechanism for accommodating tectonic extension. Recognizing the extent of magmatic stress accommodation is important in assessing seismic and volcanic risks.

A GENERAL, BUT VARIABLY EXPRESSED, association between magmatic activity and tectonic extension is recognized worldwide. The association is not uniform. In some rifts, igneous rocks are scarce or absent at the surface, but their presence at depth is suggested by the high heat flow or thermally elevated lithosphere. We suggest that in the seismogenic upper crust, two end-member processes, normal faulting and magmatic intrusion, work together to accommodate extension in varying proportion depending upon magma supply. Below the seismogenic zone, extension is accommodated primarily by ductile flow in the lower crust (*1*). The high speed that dikes propagate relative to the ductile flow rate allows them to penetrate the lower crust, which acts elastically over the short duration of intrusion.

Department of Geophysics, Stanford University, Stanford, CA 94305.

Basaltic magmatism is of particular tectonic importance because it results from partial melting in the Earth's mantle at depths where the density differences between solid and fluid can produce a large buoyant driving pressure. The low viscosity of basaltic relative to more silicic melts (*2*) causes the melts to be intruded as tabular vertical dikes or horizontal sills (*3*). Tabular intrusions are by their geometry able to affect primarily a single component of the stress field, whereas the radially symmetric intrusions produced by more viscous silicic melts tend to have a more uniform effect on the stress field.

In the brittle upper crust tectonic extension in one horizontal direction can be accommodated by normal faulting, in which vertical thinning occurs at constant volume, or by vertical dike injection perpendicular to the extension direction, which increases the rock volume. Complementary extension in one horizontal direction and contraction in another can take place by strike-slip faulting, in which both a constant surface area and constant volume are maintained. Oblique normal faulting represents hybrid behavior between these end members.

We suggest that basaltic magma supplied at a pressure greater than the least principal stress is capable of suppressing normal faulting and the earthquakes and topography that commonly accompany normal faulting. Such magma pressure would also tend to suppress strike-slip faulting.

In normal faulting, the least principal stress is horizontal and in the direction of extension (Fig. 1A). The vertical principal stress, consisting of the lithostatic load, is maximum (*4*). We follow the convention of giving compressional stress in the earth a positive sign. Normal faults fail by shear in response to this maximum principal stress (*5, 6*). Conversely dikes intrude along vertical planes of tension fracturing perpendicular to the least principal stress. In the upper crust (~15 km thick), elastic strain can be stored during slow tectonic extension and episodically released when shear strength is exceeded, a fault slips suddenly, and an earthquake is produced. During this cycle, which generally has a period of hundreds to thousands of years at any given locality, the least principal stress decreases and then suddenly increases at the moment of rupture. The vertical principal stress, governed by the lithostatic load, remains constant. In other words, the deviatoric stress reaches a maximum value and then decreases toward zero during rupture.

Rapid, episodic dike injections cause a similar cycling of stress. When a vertical dike intrudes into extending brittle crust, it pushes against its walls, in opposition to the least principal stress. For a sufficient magma pressure, inflation of vertical dikes can significantly increase the least principal stress and cause a net reduction of the deviatoric stress (Fig. 1B). The rapidity with which dikes are emplaced causes a nearly instantaneous change to the local stress field, and a single dike can accommodate hundreds to thousands of years of accumulated tectonic stress. As the least principal stress is increased, the intermediate stress (horizontal and orthogonal to the least principal stress) is also increased by a factor of Poisson's ratio (Poisson's ratio averages about 0.25 in crustal rocks). Rapid dike injection then has the effect of not only suppressing faulting (7) but also increasing both the horizontal stresses, and if the increase is large, reorienting the principal stresses. Stress reorientation is possible because the upper bound is a free surface, and thus the vertical stress is unaffected by dike injection. If the least principal stress is increased to equal the value of the intermediate stress, then an orthogonal set of vertical dikes can form. In the aggregate, generation of orthogonal dike sets should be of minor significance in the usual case of tectonic extension in one horizontal direction (uniaxial strain). The case of horizontal sheet emplacement (Fig. 1C) arises where a large supply of high-pressured magma would increase both horizontal stresses faster than can be accommodated by tectonic strain.

Significantly, in the case of a magma supply at a pressure exceeding the least principal stress, deformation occurs without the shear strength of the rock being exceeded. Extension takes place by dike injection instead of normal faulting. Magma pressure and dike injection would similarly inhibit strike-slip faulting by increasing the least principal stress and reducing the elastic strain.

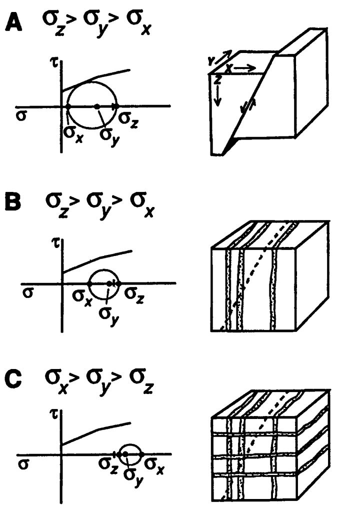

Fig. 1. Mohr-Coulomb representation of the relation between magmatism, faulting, and the stress field. The vertical axis is shear stress (τ), and the horizontal axis is confining pressure or stress (σ). The diameter of the circle is the deviatoric stress, which is the difference between the maximum and minimum principal stresses [($\sigma_z - \sigma_x$) in the case of an extending tectonic regime]. The plotted curve is the approximate Mohr failure envelope (positive quadrant plotted), which divides the zone of stability below it from the zone of failure or instability above; the break in the stability envelope represents conceptually a transition to more ductile rocks deep in the crust. (**A**) In this case the deviatoric stress is large enough for the Mohr circle to touch the failure envelope, and normal faulting ensues. (**B**) Dikes intrude on vertical planes, exploiting the weak tensile strength of the rock. As the dikes intrude, they press against their walls in the direction of extension and opposite the least principal stress. The net effect is an increase in the least principal stress, which in turn decreases the deviatoric stress; a smaller Mohr circle is generated that no longer touches the failure envelope, and normal faulting ceases. (**C**) Continued dike intrusion increases the stress in the x direction such that it is no longer the least principal stress, and the intermediate stress (σ_y) also increases by a factor of Poisson's ratio. Given a sufficient magma supply, the vertical stress could then become the least principal stress, and horizontal intrusions would be favored.

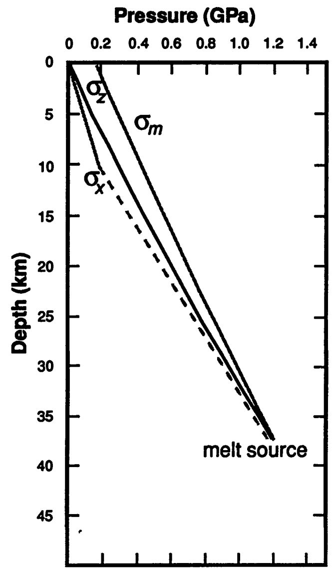

Fig. 2. Calculated magma overpressure of an example average basaltic melt composition from the Eastern Snake River Plain, Idaho (σ_m is magma pressure; σ_z is the greatest principal stress, which is vertical in an extending terrane; σ_x is the horizontal least principal stress; melt temperature is fixed at 1200 K; melt density is allowed to vary according to confining pressure). If the melt generation is assumed to occur at the lithostatic pressure ($\sigma_m = \sigma_z$) at the base of the crust, and the melt column is connected from the melt source to its final emplacement, then the internal magma pressure will exceed σ_z during its entire ascent [if viscous losses (*4, 10*) are neglected]. As long as the magma pressure exceeds σ_x, it will be overpressured, driven by the relative difference between the low-density magma and the surrounding higher density rock deep in the Earth's crust or in the mantle. Melt density changes little during its ascent, but upper crustal rocks are commonly less dense than basaltic melt. Melt is able to climb in a dike through these rocks because it is not able to penetrate the rigid walls of the dike and interact with the rocks; ascent thus continues to be driven by the density instability below. The observation that basaltic melts reach the surface in extending terranes suggests that the melt pressure exceeds lithostatic pressure and thus must exceed σ_x. This condition enables the melt to affect the stress orientations.

We assume that during incipient intergranular melting of mantle peridotite the basaltic melt is subjected to the same pressure as the enclosing rock. As melt gathers into discrete bodies, the vertical gradient of pressure in the melt is less than that in the rock because of the lower density of the melt at depth (*8, 9*) (Fig. 2). In an extending terrane, basaltic melt that was less dense than the surrounding rock at depth can climb up through upper crustal rock that is exceeded in density by the melt, as is commonly observed. The chilling viscous magma does not ordinarily penetrate the pores in the wall rock of the dike. The effect is analogous to dense mercury climbing up a glass barometer tube, pushed up by air pressure on the pool at its base. More precisely, for a vertical dike to form, the rock must be subjected to differential stress, the least principal stress must be horizontal, and the melt must have an overpressure relative to the least principal stress (*10*). Eruptions from high volcanoes and large-scale flood basalts provide ample evidence that magma overpressure is common.

The discovery of widespread diabase sheets intruded subhorizontally in the crust indicates that the magma in those localities achieved a pressure that was high enough to fracture the rock and to lift the overburden and that the least principal stress was oriented vertically at the time of emplacement. The sheets are known from drilling (*11*), seismic reflections (*12–14*) (Fig. 3) and geologic studies (*15, 16*) throughout a wide range of depths from 1 km to at least 12 km. The least principal stress must have been oriented horizontally before the formation of the sheets to allow a feeder dike to form. The occurrence of intruded sheets at different levels in the crust implies not only that the magma was overpressured but that the principal stresses were cycling between horizontal and vertical.

A full spectrum in the relations between magmatic activity and extension is seen ranging from so-called "dry rifts" with little or no surface expression of magmatism, to extended regions covered with abundant volcanic rocks. Dry rifts tend to be more seismically active and develop higher topography than those with considerable basaltic magmatism.

The East Pacific Rise is a fast spreading ridge with low topographic relief in the spreading center and is relatively aseismic compared to the Mid-Atlantic Ridge (*17–19*). Most of the

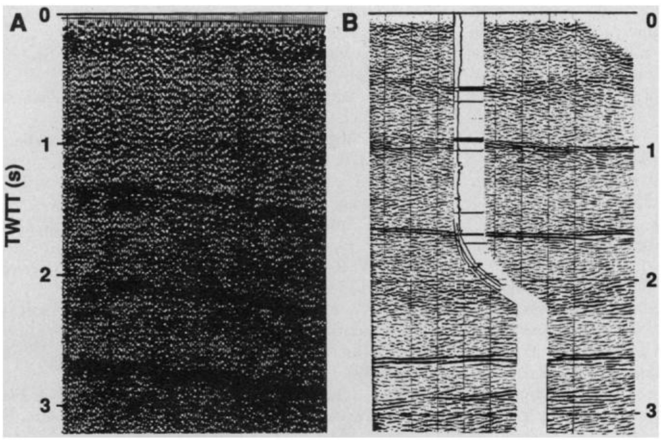

Fig. 3. Seismic reflections from diabase sheets intruded subhorizontally into crystalline rocks of (**A**) central Arizona (*12*), and (**B**) Siljan, Sweden (*11*). The sheets at Siljan were drilled and their composition confirmed. The presence of horizontally intruded sheets can be useful in determining the stress field at the time of their emplacement and in explaining contemporary seismicity. Vertical axis is travel time, which corresponds with depth.

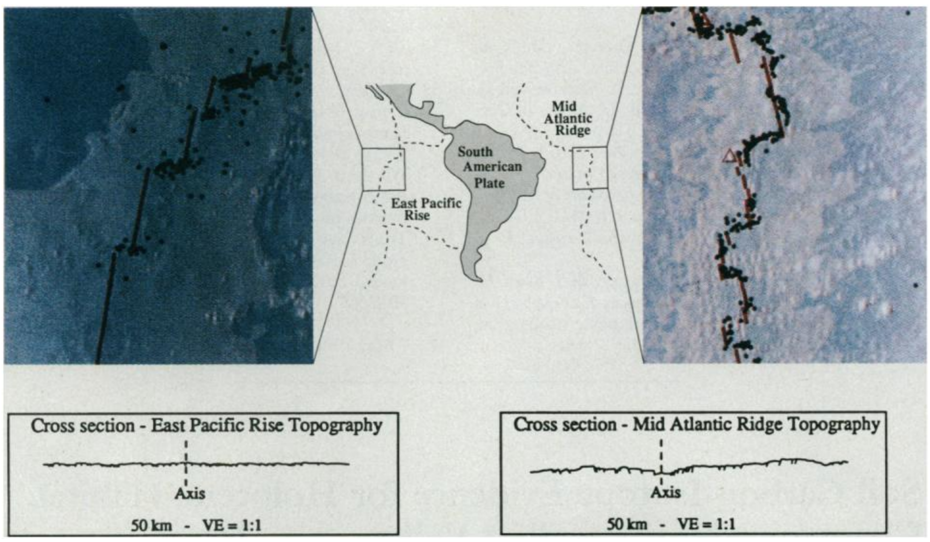

Fig. 4. A comparison of two oceanic spreading centers, the East Pacific Rise (left) and the Mid-Atlantic Ridge (right) [black dots are earthquake epicenters of magnitude ≥4.0 (*19*)]. The East Pacific Rise is spreading faster than the Mid-Atlantic Ridge, has lower topographic relief, is seismically less active, and is supplied by a larger magma chamber. The magma supply to the East Pacific Rise is probably sufficient to accommodate most of the extension, and thus normal faults like those observed on the Mid-Atlantic Ridge are unnecessary. VE, vertical exaggeration.

seismicity on the East Pacific Rise occurs on transform faults rather than on normal faults as on the Mid-Atlantic Ridge (Fig. 4) (*19, 20*). This observation suggests that increased magmatism is accommodating the extension in the Pacific and is suppressing normal faulting and associated topography.

A comparison of the eastern and western branches of the East African rift system reveals that magmatism has been much more extensive in the eastern branch than in the western branch. The western branch is essentially a dry rift and is more seismically active than the eastern branch (Fig. 5), although both branches are actively extending. Thus it appears that extension is accommodated substantially by magmatism on the eastern branch and by brittle thinning on normal faults on the western branch.

The Basin and Range Province of the western United States is a broad, block-faulted, regionally extended terrane with associated magmatism of locally variable rates and compositions. Earthquakes with magnitudes as high as 7.0 are common on normal faults. The Eastern Snake River Plain, situated near the northern edge of the Basin and Range Province, marks the track of the Yellowstone hot spot, which caused massive basaltic magmatism (*21–23*). The eastern Snake River Plain cuts an essentially aseismic (*24, 25*) (Fig. 6) swath of low topography across the characteristic block-faulted mountains of the adjacent Basin and Range Province, although the plain continues to extend longitudinally at comparable rates to the adjacent regions (*26*). Feeder vents for the basalts trend northwest-southeast across the eastern Snake River Plain; this direction is perpendicular to the extension direction and indicates that dikes at depth are accommodating extension and suppressing normal faulting and associated topography (*27*). Similar analo-

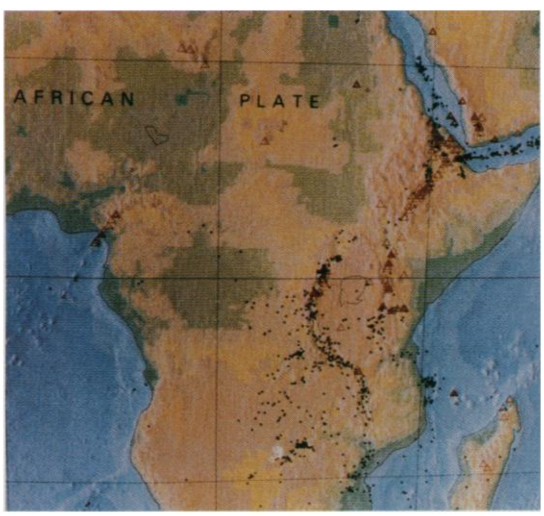

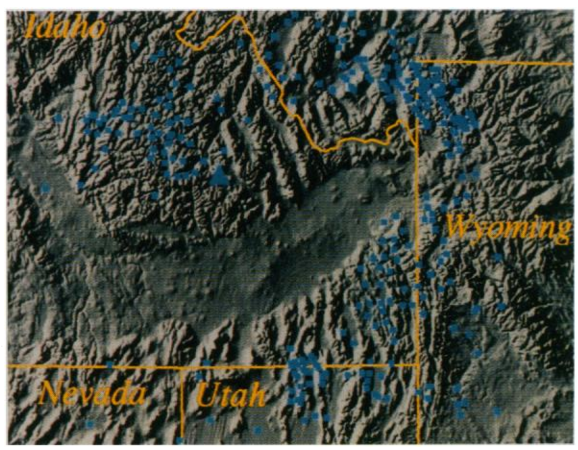

Fig. 5 (left). Seismicity and volcanic activity map of the African continent (*19*) with earthquake epicenters (magnitudes ≥4.0) plotted as black dots and volcanic events as red triangles. The eastern branch of the East African Rift (clearly outlined by increased activity) shows higher magmatism and lower seismicity than the western branch. **Fig. 6 (right).** Seismicity (earthquake magnitudes ≥3.0) overlain on the topography (*32*) of the Eastern Snake River Plain. Earthquake epicenters are plotted as blue squares, and the triangle shows the location of the 1983 magnitude 7.3 Borah Peak earthquake. The axis of the plain, where vertical dikes have fed young basalt flows on the surface, shows a dramatic lack of seismicity and topography when compared to the surrounding Basin and Range Province.

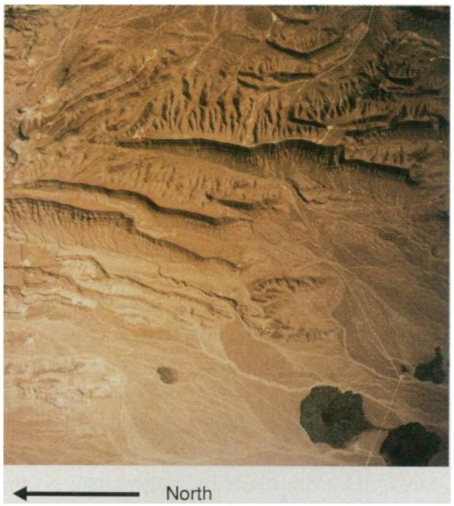

Fig. 7. Air photo of the Yucca Mountain area of southern Nevada and small-scale interaction between normal faulting and magmatic activity. The scarps of active normal faults strike toward the basaltic cones in the lower right corner, where the faults die out. Increased local magmatic input to the crust is absorbing the extension that otherwise would be accommodated by these faults.

gous regions that have holes, or low-seismic zones in the pattern of seismicity are scattered around the Basin and Range Province. The Yucca Mountain area of southern Nevada (Fig. 7), the Mono Craters of eastern California (*28*), and the Valles Caldera of New Mexico (*29*) all show a relation between young magmatism and low seismicity. Vertical intrusions are observed to be accommodating extensional strain in the Coso Mountains of California (*30, 31*).

When assessing volcanic and earthquake hazards it is important to recognize that these phenomena often occur as coupled processes and that magmatism plays an important role in relieving tectonic stresses, particularly in extending regimes. Geophysical remote sensing methods capable of detecting horizontal magmatic intrusions, as well as in situ stress measurements, offer a means of confirmation where magmatic stress accommodation is suspected. An understanding of dike and sheet emplacement may also be important for controlling massive artificial hydrofracturing, which is often used to enhance the yield of oil from reservoirs.

REFERENCES AND NOTES

1. See S. I. Kirby and A. K. Kronenberg, *Rev. Geophys.* **25**, 1219 (1987), for review and detailed references on crustal rheology.
2. M. G. Best, *Igneous and Metamorphic Petrology* (Freeman, New York, 1982).
3. S. H. Emerman and R. Marrett, *Geology* **18**, 231 (1990).
4. For simplicity we describe the stresses as if they were uniform over broad regions. We recognize, however, that dikes propagate because of the extremely nonuniform stresses at their tips [see (*5*) and D. Moos and M. D. Zoback, *J. Geophys. Res.* **95**, 9305 (1990)]. We generally do not include pore pressure in the discussion because magma does not appreciably penetrate rock pores, but in the zone of melt generation internal pore pressure of the melt fraction can reduce the effective stress and cause rocks at great depth to behave in brittle fashion.
5. A. M. Rubin and D. D. Pollard, *Geology* **16**, 413 (1988).
6. E. M. Anderson, *The Dynamics of Faulting and Dyke Formation* (Oliver and Boyd, Edinburgh, 1951).
7. M. K. Hubbert and D. G. Willis, *Trans. Am. Inst. Min. Metall. Pet. Eng.* **210**, 153 (1957).
8. N. H. Sleep, *J. Geophys. Res.* **93**, 10,225 (1988).
9. D. L. Turcotte and G. Schubert, *Geodynamics* (Wiley, New York, 1982), p. 240.
10. Intentionally not discussed here are effects of viscous loss associated with fluid flow and local stress effects associated with crack propagation such as opening and healing. Although these effects are important to understanding dike emplacement, they are of secondary importance in their contribution to the overall stress field that governs faulting, earthquakes, and topography.
11. C. Juhlin, in *Deep Drilling in Crystalline Bedrock*, A. Boden and K. G. Eriksson, Eds. (Springer-Verlag, New York, 1988), pp. 113–121.
12. E. Goodwin *et al.*, *Tectonics* **8**, 821 (1989).
13. J. McCarthy and G. A. Thompson, *Geol. Soc. Am. Bull.* **100**, 1361 (1988).
14. J. M. Howie, T. Parsons, G. A. Thompson, in *Fourth International Symposium on Deep Seismic Reflection Profiling of the Continental Lithosphere*, R. Meissner and H. Dürbaum, Eds. (*Geophys. Monog. 63*, American Geophysical Union, Washington, DC, in press).
15. C. E. Corry, *Geol. Soc. Am. Spec. Pap.* **220**, 1 (1988).
16. K. A. Howard, *J. Geophys. Res.*, in press.
17. B. Gutenberg and C. F. Richter, *Seismicity of the Earth* (Princeton Univ. Press, Princeton, NJ, ed. 2, 1954).
18. K. C. Macdonald and J. D. Mudie, *Geophys. J. R. Astron. Soc.* **36**, 245 (1974).
19. T. Simkin, R. I. Tilling, J. N. Taggart, W. J. Jones, H. Spall, *This Dynamic Planet, Volcanoes, Earthquakes, and Plate Tectonics* (Smithsonian Institution, Washington, DC, 1989).
20. B. Isacks, J. E. Oliver, L. R. Sykes, *J. Geophys. Res.* **73**, 5855 (1968).
21. W. J. Morgan, *Am. Assoc. Pet. Geol. Bull.* **56**, 230 (1972).
22. R. B. Smith and M. L. Sbar, *Geol. Soc. Am. Bull.* **85**, 1205 (1974).
23. F. C. Armstrong, W. P. Leeman, H. E. Malde, *Am. J. Sci.* **275**, 225 (1975).
24. M. H. Anders, J. W. Geissman, L. A. Piety, J. T. Sullivan, *J. Geophys. Res.* **94**, 1589 (1989).
25. R. B. Smith, W. D. Richins, D. I. Doser, *U.S. Geol. Surv. Open-File Rep.* **85-290**, 236 (1985).
26. D. W. Rodgers, W. R. Hackett, H. T. Ore, *Geology* **18**, 1138 (1990).
27. W. R. Hackett, R. P. Smith, S. M. Jackson, in preparation.
28. M. Bursik and K. Sieh, *J. Geophys. Res.* **94**, 15,587 (1989).
29. D. J. Cash and J. J. Wolff, in *Guidebook, 35th Field Conference, Rio Grande Rift: Northern New Mexico*, W. S. Baldridge, P. W. Dickerson, R. E. Riecker, J. Zidek, Eds. (New Mexico Geological Society, Socorro, 1984), pp. 25–28.
30. C. R. Bacon, *Geology* **10**, 65 (1982).
31. _____, *Geol. Soc. Am. Abstr. Program.* **15**, 288 (1988).
32. G. P. Thelin and R. Pike, *U.S. Geol. Surv. Map 12206*, in press.
33. R. Pike and G. Thelin provided their digital topographic map of the western United States (*32*) for use in figures appearing in this paper. The U.S. Department of Energy provided air photos of Yucca Mountain, NV. We thank R. Smith, W. Hackett, and S. Jackson at Idaho National Engineering Labs for cooperative discussions on crustal processes of the Snake River Plain. Thanks also to N. Sleep and the Crustal Geophysics group at Stanford for helpful discussion. This work was funded by National Science Foundation grant EAR 9017667.

7 May 1991; accepted 23 July 1991

Soil Carbon Isotope Evidence for Holocene Habitat Change in the Kenya Rift Valley

STANLEY H. AMBROSE AND NANCY E. SIKES

In eastern Africa the altitude of the boundary between montane forest and lowland savanna grassland changed substantially in response to climate change during the later Holocene, but this is not clearly reflected in regional pollen records. The carbon-13 to carbon-12 ratios of tropical grasses are higher than those of most other plants, and this difference is preserved in soil organic carbon stable isotope ratios. Soil organic matter $^{13}C/^{12}C$ ratios in profiles along an altitude transect in the central Rift Valley of Kenya suggest that the forest-savanna boundary advanced more than 300 meters in altitude. This could have implications for understanding the effects of climate change on the configuration of floral zones, prehistoric hunter-gatherer land-use patterns, and the timing of the advent of Neolithic food production.

CHANGES IN FLORAL ZONES IN East Africa during the late Quaternary have been shown by analyses of pollen from cores in swamps and lakes (*1*). Pollen provides taxonomic identifications of the composition of plant communities, but the precise location of the boundaries between major floral zones cannot be determined because of the size and altitudinal range of pollen site catchment areas. Direct identification of the past position of the boundary (ecotone) between forest and savanna in the central Rift Valley of Kenya would permit a test of arguments that the boundary was at higher altitudes during a middle Holocene arid phase; it would allow us to test a model of prehistoric human forager ecotonal settlement preferences (*2, 3*). The stable carbon isotope ratios of soil and paleosol organic matter are lower in forests than in tropical grasslands. Past changes in the position of the forest-savanna ecotone can thus be doc-

Department of Anthropology, University of Illinois, Urbana, IL 61801.